



Published in final edited form as:

Org Biomol Chem. 2009 October 07; 7(19): 4029–4036. doi:10.1039/b909729e.

Nucleoside triphosphate mimicry: a sugar triazolyl nucleoside as an ATP-competitive inhibitor of *B. anthracis* pantothenate kinase[†]

Andrew S. Rowan^a, Nathan I. Nicely^{‡,b}, Nicola Cochrane^a, Wjatschesslaw A. Wlassoff^a, Al Claiborne^b, and Chris J. Hamilton^c

^aSchool of Chemistry and Chemical Engineering, David Keir Building, Stranmillis Road, Queen's University Belfast, Belfast, BT9 5AG

^bCentre for Structural Biology, Wake Forest University School of Medicine, Winston-Salem, North Carolina 27157, USA

^cSchool of Chemical Sciences and Pharmacy, University of East Anglia, Norwich, Norfolk NR4 7TJ

Abstract

The synthesis of a library of nucleoside triphosphate mimetics is described where the Mg²⁺ chelated triphosphate sidechain is replaced by an uncharged methylenetriazole linked monosaccharide sidechain. The compounds have been evaluated as inhibitors of *Bacillus anthracis* pantothenate kinase and a competitive inhibitor has been identified with a K_i that is 3-fold lower than the K_m value of ATP.

Background

Nucleoside triphosphates (NTPs) play a critical role in a vast range of biological processes ranging from protein phosphorylation and cell signalling to DNA replication. A major challenge for the design of NTP mimetics as inhibitors of NTP-dependent enzymes (eg. kinases, DNA/RNA polymerases) is the replacement of the tetra-anionic triphosphate sidechain with a neutral, or significantly less charged, motif that will facilitate cell permeability whilst ensuring they still bind to their biological target(s) with comparable or greater efficiency than the native substrate. Most kinases/polymerases accept their incoming NTP substrates pre-coordinated to a divalent magnesium cation which is essential for substrate binding and catalysis. The divalent cation facilitates substrate binding *via* coordination to both the triphosphate ligand and carboxylate sidechains (usually aspartates) in the NTP binding domain. The design of uncharged bioisosteres of the triphosphate sidechain has so far proven to be challenging.^{1,2} However, conformationally rigidified ATP mimetics have recently been prepared using a bicyclic (ethylene bridged) oxazolidine ring structure to mimic the enzyme-bound conformation of the Mg²⁺-complexed triphosphate

[†]Electronic supplementary information (ESI) available: Additional experimental procedures for compound syntheses and characterisation data are provided in the supplementary information. See DOI: 10.1039/b909729e

[‡]Current address: Duke Human Vaccine Institute, 450 Research Drive, Durham, NC 27708, USA.

sidechain.³ In this case, an inhibitor of human tyrosine kinase (HER-2) was developed with a K_i value of 88 μM (compared to $K_m(\text{ATP})$ of 5 μM). NTPs adopt different conformations when bound to different enzymes. Molecules that mimic specific enzyme-bound conformation(s) of NTP- Mg^{2+} could help to confer inhibitor selectivity for individual (or sub-populations of) NTP-dependent enzymes.

In the sugar nucleotide arena, there have been numerous attempts to prepare uncharged pyrophosphate isosteres, but with limited success.⁴ One notable exception is lactosyl uridine **2**, where the pyrophosphate- Mn^{2+} complex of the galactosyltransferase donor substrate, uridine-5'-diphosphogalactose (UDP-Gal) **1** is replaced with a bridging 1,4- β -D-glucose linkage (Fig. 1).⁵ Lactosyl uridine, **2**, proved to be a competitive inhibitor of 1,4-GalT activity from leukemia ascites fluid with a K_i value comparable to K_m of the native substrate **1** implying that the central glucose moiety of **2** is isosteric with a pyrophosphate-metal ion complex (Fig. 1). More recently, the inhibitory effect of **2** (500 μM) against bovine β -1,4-galactosyltransferase was shown to be <10% in the presence of K_m concentrations of UDP-Gal (120 μM).⁶ This may be attributed to structural differences in GalTs from different species and in particular the gross binding conformation of their donor substrates.

Pyrophosphate mimicry by hexoses is also observed in nature. The dolichol-pyrophosphate- α -D-GlcNAc-synthase inhibitor tunicamycin uses an L-rhamnose-configured monosaccharide to mimic the pyrophosphate- Mn^{2+} complex of the natural dolichol-pyrophospho-GlcNAc substrate (Fig. 1).^{7,8} The stereo-configuration and substitution patterns of the central sugar motifs in **2** and tunicamycin significantly differ (Fig. 1). Evidently, no single monosaccharide motif can operate as a generic pyrophosphate-metal ion isostere due to different ligand-binding requirements of sugar nucleotides with different enzymes. How a neutral monosaccharide effectively mimics a charged pyrophosphate-metal ion chelate could be a combination of appropriate spacing/orientation of the terminal nucleoside and sugar motifs and interactions of the bridging glucose motif with the pyrophosphate-binding pocket. Substrate-binding interactions between the pyrophosphate-metal ion and aspartate sidechains in the pyrophosphate binding pocket could perhaps be replaced by hydrogen bonding interactions with one or more hydroxyl groups of a monosaccharide. We were curious to see if any such examples of pyrophosphate-metal ion mimicry would translate into the design of NTP mimics by replacing the terminal β, γ -pyrophosphate motif with a neutral monosaccharide.

We recently reported the preparation of sugar nucleoside monophosphates (sugar-NMPs) such as **3** and **4**, which could potentially serve as significantly less charged ATP mimics (Fig. 2).⁹ However, these sugar-NMPs still retain a charged and hydrolytically unstable glycosyl phosphate linkage. Replacing the remaining phosphate with a readily accessible *O*-methylene triazole linker (Fig. 2) would resolve these polarity/stability concerns. The viability of the triazole group as a bioisostere for the phosphate group in the sugar-phosphate backbone of nucleic acids has recently been demonstrated.¹⁰ Herein, we describe the synthesis and evaluation of a parallel library of sugar-triazole-nucleosides (STNs) as inhibitors of the type-III pantothenate kinase from *Bacillus anthracis* (BaPanK). From this library, a competitive inhibitor is identified whose K_i is 3-fold lower than K_m of the competing substrate (ATP).

Results and discussion

Chemistry

AMP-glucose **3** and AMP-galactose **4** were prepared (as anomeric mixtures) using reported methods.⁹ For construction of the sugar-triazole-nucleoside (STN) library, 5'-azido uridine **7** and 5'-azido-2-deoxythymidine **8** were prepared, in good yield, by treatment of the free nucleosides, **5** and **6** with triphenylphosphine, carbon tetrabromide and lithium azide (Scheme 1).¹¹

Similar procedures were used to access 5'-azido cytidine **11** from the N⁴-benzoyl protected derivative **9**.^{11,12} The *N*-benzoyl protecting group was employed to prevent intermolecular alkylation of the nucleobase *via* reaction with the 5'-bromo nucleoside intermediate, which is generated *in situ* prior to reaction with lithium azide. 5'-Azido adenosine **14** has previously been prepared in five steps from N⁶-benzoyl adenosine.¹³ Herein, a more succinct route involved treatment of 2',3'-*O*-isopropylidene adenosine **12** with diphenyl phosphoryl azide, diisopropylazodicarboxylate and triphenylphosphine to give **13**.¹⁴ The isopropylidene protecting group served to enhance the solubility of **13**, which facilitated purification by column chromatography prior to its removal under acidic conditions to give **14**. A variety of methods were employed to access the different propargyl glycosides. Alpha-propargyl glycosides of D-Glc **15**,¹⁵ D-GlcNAc **16**,¹⁶ D-Man **17**¹⁷ and D-Xyl **19** were all obtained using acid catalysed Fischer glycosylation conditions (Scheme 2). The same conditions were used to prepare *O*-propargyl derivatives of L-Ara **18** and D-Gal **20** as anomeric mixtures, which were inseparable by chromatography. However, for **20** the 4,6-*O*-benzylidene acetal derivatives, **21** and **22**, were separable by chromatography enabling access to the desired α -galactoside **23**.

Treatment of peracetylated D-Rib **24**, D-Gal **27a** and D-Xyl **28a** with propargyl alcohol in the presence of BF₃·OEt¹⁸ was used to access the β -propargyl glycosides **26**, **27c**, **28c** (Scheme 3).

The β -propargyl glycoside of GlcNAc **31** was accessed *via* silver triflate promoted glycosylation of propargyl alcohol with glycosyl bromide **29** (Scheme 4a).¹⁹ Similar procedures were employed to access glucosamine derivative **35** (Scheme 4b). Preparation of 2-azido-2-deoxy- α -D-glucopyranosyl bromide **33** by treatment of peracetylated precursor **32** with HBr in glacial acetic acid was unsuccessful, providing a complex mixture of products (by TLC). An alternative treatment with titanium(IV) bromide²⁰ gave the desired beta-anomer in 31% yield (40% of unreacted starting material was also recovered during chromatography). Reaction of **33** with propargyl alcohol in the presence of silver triflate provided propargyl glycoside **34** in good yield as an anomeric mixture (α : β ratio = 1:1.1). Subsequent deacetylation under Zemplén conditions in a sonicator²¹ rapidly proceeded to completion in just three minutes.

Amino-sugar **36** could not be accessed by hydrogenation of azido-sugar **35** as this would also have reduced the alkyne, hence alternative methods were explored. Under Staudinger conditions (with tributylphosphine) the azide moiety of **35** was not reduced and only

unreacted starting material was recovered. However treatment with zinc and ammonium chloride²² reduced the azide whilst leaving the alkyne aglycone intact.

The thymidine STNs **49–59** were the first to be prepared using the copper(I)-catalysed [3 + 2] azide-alkyne cycloaddition (Cu-ACC) reaction between the aforementioned propargyl glycosides and azido-nucleoside **8** in the presence of copper sulfate and sodium ascorbate (Scheme 5, Table 1).²³ Under these conditions, reactions took 1–3 days to reach completion (by TLC). For the adenosine, uridine and cytidine derivatives **37–48** and **60–81**, alternative reaction conditions using copper(I) bromide, *tris*-(benzyltriazolylmethyl)amine (TBTA),²⁴ under sonication²¹ gave improved yields and shorter reaction times (30–40 minutes).

Enzyme assays

The type-III pantothenate kinase from *Bacillus anthracis* (*BaPanK*) was used to study the NTP mimicry of all the STNs that were made. Pantothenate kinase (PanK) catalyses the first obligate step in Coenzyme A biosynthesis, namely the ATP-dependent phosphorylation of pantothenic acid (Scheme 6a). To date, the crystal structures of type-III PanK enzymes from *Thermotoga maritima* (*TmPanK*),^{25,26} *Pseudomonas aeruginosa* (*PaPanK*)²⁷ and *BaPanK*²⁸ have been reported, but co-crystallisation of any of these Mg²⁺-dependent enzymes with ATP-Mg²⁺ has not yet been accomplished. Type-III PanK enzymes exhibit unusually high K_m values of 3–10 mM^{29,25,27} compared to K_m (ATP) values of <200 μ M generally observed with PanK types I and II. Some type III panKs also display a broad tolerance for other NTPs as alternative phosphate donor substrates.^{27,29} For Type-III PanKs, the nucleobase end of the ATP binding site is open to the solvent and doesn't support tight binding interactions with the adenosyl nucleobase, as shown by active site docking of the inert substrate mimic adenosine 5'-(β , γ -imido)triphosphate (AMPPNP) with *PaPanK*²⁷ and the structure of the ADP:pantothenate ternary complex with *TmPanK*.²⁶ For the studies reported herein, *BaPanK* activity/inhibition was monitored using a coupled assay as outlined in Scheme 6b.

BaPanK is able to utilise a range of NTPs as phosphate donors (Table 2). The catalytic efficiencies (k_{cat}/K_m) of the purine NTPs (ATP, dATP, dGTP) were 5–10-fold greater than their pyrimidine counterparts. This is primarily due to their lower K_m values whereas the steady state turnover rates (k_{cat}) of the pyrimidines were much closer to (and in some cases better than) those of the purine NTPs. The K_m (ATP) for *BaPanK* (510 μ M) is significantly lower than those reported for other type-III PanKs (3–10 mM).^{25–27,29} It is interesting to note that removal of the 2'-hydroxyl on the ribose ring leads to reductions in both K_m and k_{cat} , but with no significant overall reduction in catalytic efficiency (k_{cat}/K_m). The K_m value for pantothenate is 275 (\pm 11) μ M. All of the NTPs in Table 2 have previously been evaluated as substrates for *PaPanK* where a preference for purine NTPs was also observed.¹⁸ However, a direct qualitative comparison cannot be made because the NTP specificity of *PaPanK* was determined from relative enzyme activity measurements in the presence of a fixed concentration of the different NTPs (250 μ M). Not all type-III enzymes share the same NTP substrate promiscuity. As well as ATP, *HpPanK* can also utilise GTP and CTP (but not UTP), whereas *BsPanK* cannot utilise any of these three alternative phosphate donors.²⁰

Compounds **37–81** were screened (at 1 mM concentrations) for BaPanK inhibition in the presence of ATP (125 μ M) and pantothenate (250 μ M). High inhibitor and low ($<K_m$) ATP concentrations were chosen to ensure that even moderate ATP-competitive inhibitors wouldn't go unnoticed. Under these conditions the majority of the STNs displayed no significant (ie. $<20\%$) inhibition (Table 1). Compounds **52**, **69**, **73** and **79** proved to be false positives due to inhibition of the coupled enzymes (PK and/or LDH). Similar inhibitory effects on the coupled enzymes were also observed for the sugar-NMPs **3** and **4**.

The β -galacto-configured adenosyl STN **40** displayed 96% inhibition of BaPanK activity under these assay conditions, but did not inhibit the PK/LDH coupled enzymes during control experiments. Detailed analysis showed **40** to be a competitive inhibitor of BaPanK (with respect to ATP) with a K_i of 164 μ M (Fig. 3). This suggests that, for this enzyme, **40** operates as an ATP mimetic, which, despite lacking all of the negative charges of the parent triphosphate, has a K_i that is 3-fold lower than the K_m value of the competing substrate (ATP). The anomeric configuration of the sugar-triazole sidechain is important as the α -galacto-configured adenosyl STN **39** shows no inhibitory activity. The axial configuration of the 4-hydroxyl of the galactose moiety is also of great importance as the gluco-configured epimer **38** was inactive. The anomeric mixture of L-arabino-configured ATP mimic **46** (with an axial 4-hydroxyl group) displayed 24% inhibition at 1 mM concentrations (Table 1). Based on the structure–activity data for **38–40**, it is likely that the β -anomer is the active component of **46**. The K_m values for UTP, CTP and dTTP are, at most, only 3.5-fold greater than that of ATP (Table 2). Hence, the lack of any significant activity with the β -galacto-configured pyrimidines **52**, **63**, **74** (Table 1) suggests that the adenine nucleobase also makes a notable contribution to the efficacy of **40**. In the absence of a type-III PanK structure co-crystallised with ATP, Mg^{2+} and the additional monovalent cation, reasons for inhibition by the β -galacto-configured STN **40** are not immediately clear. The structure of the ADP:pantothenate ternary complex with *Tm*PanK shows how ATP- Mg^{2+} must bind in an extended conformation during the catalytic pathway.²⁶ The loss of inhibitory activity going from the β -galactoside **40** to its α -anomer **39** could be the consequence of **40** being able to adopt such an extended conformation whereas its α -configured diastereoisomer **39** would be bent into a disfavourable orientation at the anomeric linkage. Evidently, the axial hydroxyl of the galactose portion of **40** plays a significant role in inhibitor recognition. Using Autodock (4.0.1),²² it has not been possible to predict a satisfactory binding orientation for **40** with the BaPanK apo-enzyme¹⁹ where inversion of the axial hydroxyl (ie. to **38**) results in a significant loss of binding interactions and/or steric clashing that could plausibly account for the significant loss of inhibitor activity with **38** (data not shown). For future consideration, co-crystallisation studies of **40** with BaPanK would help establish the binding orientation of **40** as well as if/how the β -linked galacto-motif is able to mimic the β,γ -pyrophosphate portion of ATP with this enzyme.

Conclusions

This study demonstrates how effective ATP mimics can be prepared where the charged triphosphate sidechain is replaced by an uncharged monosaccharide and that small variations in the monosaccharide stereoconfiguration lead to dramatic changes in inhibitor potency. It

will be interesting to evaluate and compare the structure–activity relationship of this STN library with other NTP-dependent enzymes. More detailed mechanistic studies with *BaPank*, and other kinases, are ongoing and will be reported in due course.

Experimental

General

^1H and ^{13}C NMR spectra were obtained using Bruker AV 300, DPX 300 or DRX 500 NMR spectrometers. Chemical shifts are quoted in parts per million (δ) using the residual solvent peak as an internal reference. IR spectra were recorded on a Perkin-Elmer RX I FT-IR system. Optical rotations ($[\alpha]_{\text{D}}$) were obtained with a Perkin-Elmer Model 341 Polarimeter, using the specified solvent and concentration, and are quoted in units of $10^{-1}\text{deg cm}^2 \text{g}^{-1}$. Thin layer chromatography (TLC) was carried out on Macherey-Nagel SIL G-25 UV₂₅₄ glass-backed silica plates, which were visualised using a UV lamp, basic potassium permanganate solution or sulfuric acid (10% (v/v) in ethanol). Flash chromatography was carried out using Fluorochem silica gel for flash chromatography. Automated flash chromatography was performed on a Biotage Horizon or Biotage SP1 HPFC system using Si 12 + M or Si 40 + M pre-packed cartridges. Dry pyridine was purchased from Fluka, and other solvents were dried using a Braun 1 solvent purification system. Sonication-mediated reactions were carried out using a Branson model 2510 sonicator bath operating at a frequency of 40 kHz. TBTA was made as previously described.²⁴ Propyl-2-ynyl- β -D-glucopyranoside was purchased from Aldrich. Recombinant *BaPank* was overexpressed and purified as previously described.²⁸ Rabbit muscle pyruvate kinase (PK) and rabbit muscle lactate dehydrogenase (LDH) were purchased from Sigma. Enzyme assays were carried out using either a PerkinElmer UV Lambda 25 spectrophotometer or a Tecan Saffire microplate reader. Compounds **7**,¹¹ **8**,¹¹ **11**,¹¹ **13**,¹⁴ **27a**,¹⁸ **27b**,¹⁸ **29**,¹⁹ and **32**³⁰ were prepared following published methods. Representative procedures are described below for the preparation of STNs **40**, **46**, **50**, **65** and **78**. Experimental methods and characterisation data for other STNs and all other synthetic intermediates are provided in the supplementary material.[†]

5'-Deoxy-5'-[4-(β -D-galactopyranosyloxymethyl)-1,2,3-triazol-1-yl]adenosine (40**)**—Prop-2-ynyl- β -D-galactopyranoside **27c** (28.5 mg, 0.131 mmol) and 5'-azido-5'-deoxyadenosine **14** (42 mg, 0.144 mmol) were measured into a sample vial, followed by copper(I) bromide (1 mg, 6.6 μmol). Aqueous sodium ascorbate solution (40 mM, 332 μL , 13.3 μmol) and a solution of TBTA in acetonitrile (20 mM, 333 μL , 6.6 μmol) was added, followed by methanol (700 μL), acetonitrile (367 μL) and water (368 μL). The sample vial was sealed, the lid pierced with a syringe needle, and the reaction mixture was sonicated for 30 minutes. This was concentrated in vacuo and purified by automated chromatography (EtOAc/MeOH 7:3 as eluent) to give **40** (55 mg, 82%) as a white solid: $[\alpha]_{\text{D}}^{20} = +2.3$ ($c = 1.48$, DMSO); δ_{H} (500 MHz, CD_3OD) 8.17 (s, 1H, H-2), 7.86, 7.85 ($2 \times$ s, 2H, H-8, H-5'''), 5.99 (d, 1H, J 4.5, H-1'), 4.96 (d, 1H, J 12.0, OCH_AH_B), 4.88 (dd, 1H, J 14.5, 4.5, H-5'a),

[†]Electronic supplementary information (ESI) available: Additional experimental procedures for compound syntheses and characterisation data are provided in the supplementary information. See DOI: 10.1039/b909729e

4.79 (dd, 1H, J 14.5, 3.5, H-5' b), 4.67 (d, 1H, J 12.0, OCH_AH_B), 4.44 (t, 1H, J 5.5, H-3'), 4.38 (m, 1H, H-4'), 4.34 (d, 1H, J 8.0, H-1''), 4.29 (t, 1H, J 5.0, H-2'), 3.84 (dd, 1H, J 3.5, 1.0, H-4''), 3.78 (dd, 1H, J 11.5, 7.0, H-6'' a), 3.72 (dd, 1H, J 11.5, 5.0, H-6'' b), 3.58 (dd, 1H, J 9.5, 7.5, H-2''), 3.55 (ddd, 1H, J 7.0, 4.5, 1.0, H-5''), 3.50 (dd, 1H, J 10.0, 3.5, H-3''); δ_C (125 MHz, CD₃OD) 157.30 (C-6), 154.19 (C-2), 150.60 (C-4), 145.77 (C-4'''), 141.25 (C-8), 127.13 (C-5'''), 120.29 (C-5), 104.51 (C-1''), 90.10 (C-1'), 83.54 (C-4'), 76.93 (C-5''), 74.85, 74.81 (C-2', C-3''), 72.39 (C-2''), 71.91 (C-3'), 70.57 (C-4''), 63.03 (CH₂), 62.67 (C-6''), 52.01 (C-5'); HRMS (ES⁻) m/z calc. for C₁₉H₂₅N₈O₉ (M - H⁺): 509.1744; found 509.1758; m/z 509 (5%, M - H⁺).

5'-Deoxy-5'-[4-(L-arabinopyranosyloxymethyl)-1,2,3-triazol-1-yl]adenosine (46)

—Was prepared from an anomeric mixture of prop-2-ynyl- α/β -L-arabinopyranoside **18** (27.4 mg, 0.146 mmol) and 5'-azido-5'-deoxyadenosine **14** (46.8 mg, 0.160 mmol) as described for **40**. Following automated chromatography (EtOAc/MeOH 7:3 as eluent), **46** (59 mg, 84%) was obtained as a white solid with an α/β ratio of 1:3: $[\alpha]_D^{20} = +92.2$ (c = 1.19, DMSO); δ_H (500 MHz, DMSO-*d*₆) 8.15, 8.14, 8.06, 7.95, 7.92 (5 × s, 6H, H-2 α , H-2 β , H-8 α , H-8 β , H-5'' α , H-5'' β), 5.89 (d, 2H, H-1' α , H-1' β), 4.80–4.67 (m, 6H, H-1'' β , H-5' $\alpha\alpha$, H-5' $\alpha\beta$, H-5' $\alpha\alpha$, H-5' $\beta\alpha$, OCH_AH_B α), 4.57 (d, 1H, J 12.5, OCH_AH_B β), 4.53 (t, 2H, J 5.0, H-2' α , H-2' β), 4.48 (d, 1H, J 12.5, OCH_AH_B α), 4.42 (d, 1H, J 12.0, OCH_AH_B β), 4.30–4.20 (m, 4H, H-3' α , H-3' β , H-4' α , H-4' β), 4.17–4.13 (m, 1H, H-1'' α), 3.72–3.50 (m, 6H, H-2'' β , H-3'' β , H-4'' α , H-4'' β , H-5'' $\alpha\alpha$, H-5'' β), 3.44–3.38 (m, 1H, H-5'' $\beta\beta$), 3.38–3.32 (m, 1H, H-5'' $\beta\alpha$), 3.32–3.28 (m, 2H, H-2'' α , H-3'' α); δ_C (125 MHz, DMSO-*d*₆) 156.06 (C-6), 153.10 (C-2), 149.47 (C-4 α), 149.42 (C-4 β), 143.99 (C-4'' β), 143.89 (C-4'' α), 140.16 (C-8 α), 140.02 (C-8 β), 125.34 (C-5'''), 119.09 (C-5), 102.56 (C-1'' α), 99.17 (C-1'' β), 87.97 (C-1' β), 87.85 (C-1' α), 82.56 (C-4' α), 82.41 (C-4' β), 72.85 (C-2' β), 72.76 (C-2' α), 72.53 (C-2'' α), 70.94 (C-3' α), 70.90 (C-3' β), 70.56 (C-3'' α), 69.02 (C-2'' β), 68.64 (C-4'' β), 68.44 (C-3'' β), 67.71 (C-4'' α), 65.55 (C-5'' α), 63.37 (C-5'' β), 61.14 (CH₂ α), 60.37 (CH₂ β), 51.49 (C-5' α), 51.36 (C-5' β); HRMS (ES⁺) m/z calc. for C₁₈H₂₅N₈O₈ (M + H⁺): 481.1795; found 481.1787; m/z 983 (44%, 2M + Na⁺), 961 (8%, 2M + H⁺), 503 (32%, M + Na⁺), 481 (100%, M + H⁺).

5'-Deoxy-5'-[4-(β -D-glucopyranosyloxymethyl)-1,2,3-triazol-1-yl]thymidine (50)

—Prop-2-ynyl- β -D-glucopyranoside (23.5 mg, 0.108 mmol) and 5'-azido-5'-deoxythymidine **8** (31.7 mg, 0.119 mmol) were dissolved in MeOH (2 mL). Aqueous CuSO₄ solution (0.05 M, 110 μ L, 5.5 μ mol) was added followed by aqueous sodium ascorbate solution (0.1 M, 110 μ L, 11.0 μ mol). This was stirred for 44 hrs then concentrated in vacuo and purified by automated chromatography (EtOAc/MeOH 3:1 as eluent) to give **50** (46 mg, 88%) as a white solid: $[\alpha]_D^{20} = +23.7$ (c = 0.99, MeOH); δ_H (500 MHz, CD₃OD) 8.03 (s, 1H, H-5'''), 7.24 (d, 1H, J 1.0, H-6), 6.19 (t, 1H, J 7.0, H-1'), 4.97 (d, 1H, J 12.5, OCH_AH_B), 4.77 (d, 1H, J 12.5, OCH_AH_B), 4.78 (dd, 1H, J 14.5, 4.0, H-5'a), 4.70 (dd, 1H, J 14.5, 6.5, H-5'b), 4.41 (dt, 1H, J 6.0, 5.0, H-3'), 4.37 (d, 1H, J 7.5, H-1''), 4.15 (dt, 1H, J 7.0, 4.5, H-4'), 3.88 (dd, 1H, J 12.5, 2.0, H-6'' a), 3.66 (dd, 1H, J 12.0, 6.0, H-6'' b), 3.34 (t, 1H, J 9.0, H-3''), 3.29–3.26 (m, 2H, H-4'', H-5''), 3.20 (dd, 1H, J 9.0, 7.5, H-2''), 2.27 (dd, 2H, J 6.5, 6.0, H-2'), 1.89 (d, 3H, J 1.0, CH₃); δ_C (125 MHz, CD₃OD) 166.38 (C-4), 152.22 (C-2), 145.83 (C-4'''), 138.28 (C-6), 126.56 (C-5'''), 112.02 (C-5), 103.66 (C-1''), 87.00

(C-1'), 85.47 (C-4'), 78.11, 78.03 (C-3'', C-5''), 75.06 (C-2''), 72.40 (C-3'), 71.67 (C-4''), 63.03 (CH₂), 62.92 (C-6''), 52.59 (C-5'), 39.56 (C-2'), 12.56 (CH₃); HRMS (ES⁺) *m/z* calc. for C₁₉H₂₈N₅O₁₀ (M + H⁺): 486.1831; found 486.1833; *m/z* 524 (19%, M + K⁺), 508 (32%, M + Na⁺).

5'-Deoxy-5'-[4-(α -D-xylopyranosyloxymethyl)-1,2,3-triazol-1-yl]uridine (65)—

Was prepared from prop-2-ynyl- α -D-xylopyranoside **19** (27.7 mg, 0.147 mmol) and 5'-azido-5'-deoxyuridine **7** (43.6 mg, 0.162 mmol) as described for **40**. Following automated chromatography (EtOAc/MeOH 4:1 as eluent), **65** (63 mg, 94%) was obtained as a white solid: $[\alpha]_D^{20} = +107.7$ (*c* = 0.76, DMSO); δ_H (500 MHz, CD₃OD) 8.04 (s, 1H, H-5''), 7.40 (d, 1H, *J* 8.0, H-6), 5.73–5.70 (m, 2H, H-1', H-5), 4.86 (d, 1H, *J* 3.5, H-1''), 4.82 (dd, 1H, *J* 14.5, 3.5, H-5'a), 4.80 (d, 1H, *J* 12.5, OCH_AH_B), 4.73 (dd, 1H, *J* 15.0, 7.0, H-5'b), 4.64 (d, 1H, *J* 12.5, OCH_AH_B), 4.25 (dt, 1H, *J* 6.5, 3.5, H-4'), 4.19 (dd, 1H, *J* 5.5, 4.0, H-2'), 4.11 (t, 1H, *J* 6.0, H-3'), 3.59–3.53 (m, 2H, H-3'', H-5''a), 3.52–3.43 (m, 2H, H-4'', H-5''b), 3.38 (dd, 1H, *J* 9.0, 3.5, H-2''); δ_C (125 MHz, CD₃OD) 166.15 (C-4), 152.08 (C-2), 145.72 (C-4'''), 143.44 (C-6), 126.62 (C-5'''), 103.12 (C-5), 100.06 (C-1''), 93.41 (C-1'), 83.00 (C-4'), 75.16 (C-3''), 74.19 (C-2'), 73.59 (C-2''), 71.95 (C-3'), 71.56 (C-4''), 63.34 (C-5''), 61.60 (CH₂), 52.52 (C-5'); HRMS (ES⁻) *m/z* calc. for C₁₇H₂₂N₅O₁₀ (M-H⁺): 456.1367; found 456.1364; *m/z* 456 (100%, M - H⁺).

5'-Deoxy-5'-[4-(2-acetyl-amino-2-deoxy- α -D-glucopyranosyloxymethyl)-1,2,3-triazol-1-yl]cytidine (78)—

Was prepared from prop-2-ynyl-2-acetyl-amino-2-deoxy- α -D-glucoside **16** (31.2 mg, 0.120 mmol) and 5'-azido-5'-deoxycytidine **1** (35.5 mg, 0.132 mmol) as described for **40**. Following automated chromatography (EtOAc/MeOH 7:3 as eluent), **78** (53 mg, 83%) was obtained as a white solid: δ_H (500 MHz, CD₃OD) 8.02 (s, 1H, H-5'''), 7.35 (d, 1H, *J* 7.5, H-6), 5.87 (d, 1H, *J* 7.5, H-5), 5.71 (d, 1H, *J* 3.5, H-1'), 4.87 (d, 1H, *J* 3.5, H-1''), 4.84 (dd, 1H, *J* 14.5, 3.5, H-5'a), 4.81 (d, 1H, *J* 12.5, OCH_AH_B), 4.74 (dd, 1H, *J* 15.0, 7.0, H-5'b), 4.62 (d, 1H, *J* 12.5, OCH_AH_B), 4.26 (dt, 1H, *J* 7.0, 3.5, H-4'), 4.21 (dd, 1H, *J* 6.0, 3.5, H-2'), 4.08 (dd, 1H, *J* 7.0, 6.0, H-3'), 3.91 (dd, 1H, *J* 11.0, 3.5, H-2''), 3.83 (dd, 1H, *J* 12.0, 2.0, H-6''a), 3.69 (dd, 1H, *J* 12.0, 5.5, H-6''b), 3.66 (dd, 1H, *J* 10.5, 8.5, H-3''), 3.62 (ddd, 1H, *J* 9.5, 5.5, 2.0, H-5'''), 3.36 (dd, 1H, *J* 10.0, 9.0, H-4''), 1.94 (s, 3H, CH₃); δ_C (125 MHz, CD₃OD) 173.79 (C=O), 167.78 (C-4), 158.15 (C-2), 145.42 (C-4'''), 143.67 (C-6), 126.50 (C-5'''), 98.06 (C-1''), 96.37 (C-5), 94.83 (C-1'), 82.76 (C-4'), 74.70 (C-2'), 74.30 (C-5''), 72.77 (C-3''), 72.38 (C-4''), 72.16 (C-3'), 62.81 (C-6''), 61.27 (CH₂), 55.31 (C-2''), 52.62 (C-5'); HRMS (ES⁺) *m/z* calc. for C₂₀H₃₀N₇O₁₀ (M + H⁺): 528.2054; found 528.2051; *m/z* 550 (25%, M + Na⁺), 528 (100%, M + H⁺).

Enzyme assays

All enzyme assays were carried out at 37 °C in buffer containing HEPES (200 mM), MgCl₂ (10 mM) and NH₄Cl (60 mM), the pH of which was adjusted to 7.6 by careful addition of saturated NaOH solution.

Inhibition assays were carried out in a final volume of 1000 μ L in disposable cuvettes containing NADH (150 μ M), PEP (2 mM), pantothenate (250 μ M), ATP (125 μ M), *Ba*PanK (7.5 μ g), PK (7.5 units), LDH (15 units) plus inhibitor (1 mM). Reactions were initiated by

the addition of *BaPanK*. Inhibitor stock solutions were prepared in DMSO and all assay mixtures contained a final quantity of 4% (v/v) DMSO. Compounds showing greater than 20% inhibition were further evaluated under the same assay conditions but using twice as much PK and LDH. Compounds which showed a decrease in % inhibition under these conditions were deemed false positives (ie. inhibitors of PK and/or LDH). For K_i determinations, assays were carried out at six ATP concentrations ($0.5-2 \times K_m$) in the presence of three different concentrations of inhibitor. Initial rates were measured from the linear region of product formation and K_i values were determined by weighted non-linear regression analysis of the hyperbola plot of rate against substrate concentration using the equation for linear competitive inhibition in Grafit version 5 (Erithacus Software Ltd).

NTP substrate kinetics were carried out in a final volume of 300 μ L in a 96-well microplate. For the K_m determination of ATP, each reaction mixture contained NADH (150 μ M), PEP (2 mM), Pan (250 μ M), *BaPanK* (2.5 μ g), PK (2.5 units), LDH (5 units), and varying concentrations of ATP substrate. Reactions were initiated by addition of *BaPanK*. The same conditions were used for alternative NTP substrates except 12.5 units of PK was used to ensure that PK was not the rate limiting step in these coupled assays (as was observed when 2.5 units of PK were used). Kinetic data were analysed (by non-linear regression) using Grafit.

Supplementary Material

Refer to Web version on PubMed Central for supplementary material.

Acknowledgments

We are thankful for financial support from the Wellcome Trust (grant ref. 067525/Z/02/Z and VS/07/QUEB/A5) (WAW, CJH, NC), the Department of Employment and Learning (ASR), the National Institutes of Health (grant ref. GM-35394 (NIN, AC)) and a grant from the Southeast Regional Centre of Excellence for Biodefense and Emerging Infections. We also thank the Engineering and Physical Sciences Research Council (EPSRC) Mass Spectrometry Service Centre, Swansea, for invaluable support.

Notes and references

1. Goldring AO, Balzarini J, Gilbert IH. *Bioorg Med Chem Lett*. 1998; 8:1211–1214. [PubMed: 9871737]
2. Goldring AO, Gilbert IH, Mahmood N, Balzarini J. *Bioorg Med Chem Lett*. 1996; 6:2411–2416.
3. Liu F, Johnson EF, Austin DJ, Anderson KS. *Bioorg Med Chem Lett*. 2003; 13:3587–3592. [PubMed: 14505676]
4. Compain P, Martin OR. *Bioorg Med Chem*. 2001; 9:3077–3092. [PubMed: 11711283]
5. Wang R, Steensma DH, Takaoka Y, Yun JW, Kajimoto T, Wong CH. *Bioorg Med Chem*. 1997; 5:661–672. [PubMed: 9158864]
6. Ballell L, Young RJ, Field RA. *Org Biomol Chem*. 2005; 3:1109–1115. [PubMed: 15750655]
7. Heifetz A, Keenan RW, Elbein AD. *Biochemistry*. 1979; 18:2186–2192. [PubMed: 444447]
8. Kimura K, Bugg TDH. *Nat Prod Rep*. 2003; 20:252–273. [PubMed: 12735700]
9. Wlassof AW, Finlay RMJ, Hamilton CJ. *Synth Commun*. 2007; 37:2927–2934.
10. Isobe H, Fujino T, Yamazaki N, Guillot-Nieckowski M, Nakamura E. *Org Lett*. 2008; 10:3729–3732. [PubMed: 18656947]
11. Yamamoto I, Sekine M, Hata T. *J Chem Soc, Perkin Trans. 1*; 1980:306–310.
12. Ludwig PS, Schwendener RA, Schott H. *Synthesis*. 2002:2387–2392.

13. Wang T, Lee HJ, Tosh DK, Kim HO, Pal S, Choi S, Lee Y, Moon HR, Zhao LX, Lee KM, Jeong LS. *Bioorg Med Chem Lett*. 2007; 17:4456–4459. [PubMed: 17582766]
14. Comstock LR, Rajski SR. *Tetrahedron*. 2002; 58:6019–6026.
15. Blinkovsky AM, Dordick JS. *Tetrahedron: Asymmetry*. 1993; 4:1221–1228.
16. Yeoh KK, Butters TD, Wilkinson BL, Fairbanks AJ. *Carbohydr Res*. 2009; 344:586–591. [PubMed: 19233348]
17. Hasegawa T, Numata M, Okumura S, Kimura T, Sakurai K, Shinkai S. *Org Biomol Chem*. 2007; 5:2404–2412. [PubMed: 17637960]
18. Mereyala HB, Gurralla SR. *Carbohydr Res*. 1998; 307:351–354.
19. Gillard JW, Israel M. *Tetrahedron Lett*. 1981; 22:513–516.
20. Krist P, Kuzma M, Pelyvas IF, Simerska P, Kren V. *Coll Czech Chem Commun*. 2003; 68:801–811.
21. Deng SL, Gangadharmath U, Chang CWT. *J Org Chem*. 2006; 71:5179–5185. [PubMed: 16808504]
22. Lin WQ, Zhang XM, Ze H, Yi J, Gong LZ, Mi AQ. *Synth Commun*. 2002; 32:3279–3284.
23. Rostovtsev VV, Green LG, Fokin VV, Sharpless KB. *Angew Chem, Int Ed*. 2002; 41:2596–2599.
24. Chan TR, Hilgraf R, Sharpless KB, Fokin VV. *Org Lett*. 2004; 6:2853–2855. [PubMed: 15330631]
25. Yang K, Eyobo Y, Brand LA, Martynowski D, Tomchick D, Strauss E, Zhang H. *J Bacteriol*. 2006; 188:5532–5540. [PubMed: 16855243]
26. Yang K, Strauss E, Huerta C, Zhang H. *Biochemistry*. 2008; 47:1369–1380. [PubMed: 18186650]
27. Hong BS, Yun MK, Zhang YM, Chohnan S, Rock CO, White SW, Jackowski S, Park HW, Leonardi R. *Structure*. 2006; 14:1251–1261. [PubMed: 16905099]
28. Nicely NI, Parsonage D, Paige C, Newton GL, Fahey RC, Leonardi R, Jackowski S, Mallett TC, Claiborne C. *Biochemistry*. 2007; 46:3234–3245. [PubMed: 17323930]
29. Brand LA, Strauss E. *J Biol Chem*. 2005; 280:20185–20188. [PubMed: 15795230]
30. Liu JJ, Numa MMD, Liu HT, Huang SJ, Sears P, Shikhman AR, Wong CH. *J Org Chem*. 2004; 69:6273–6283. [PubMed: 15357586]

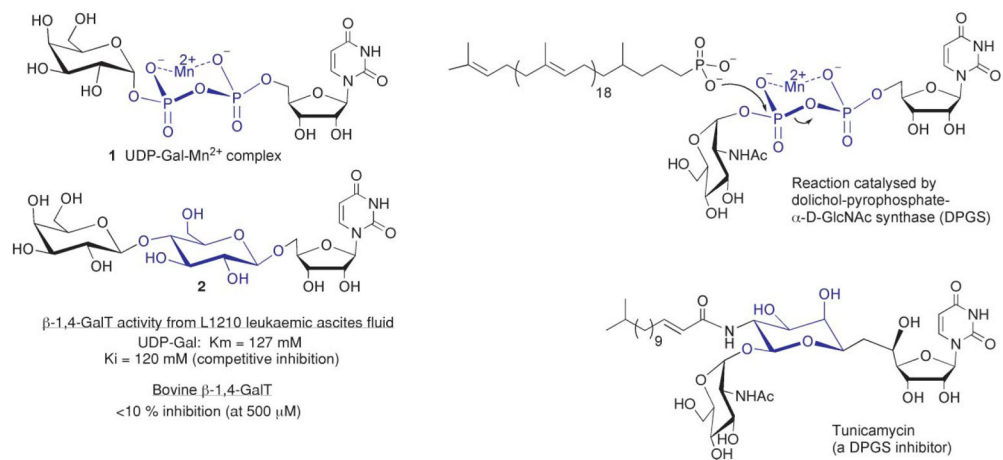


Fig. 1.
 Examples of pyrophosphate-M²⁺ mimicry by monosaccharides.

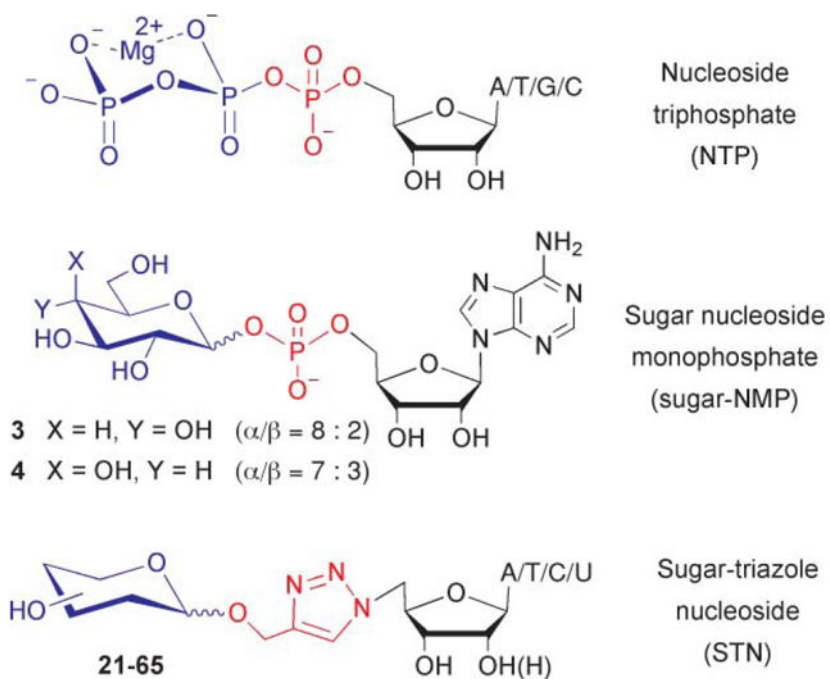


Fig. 2.
Proposed NTP mimics.

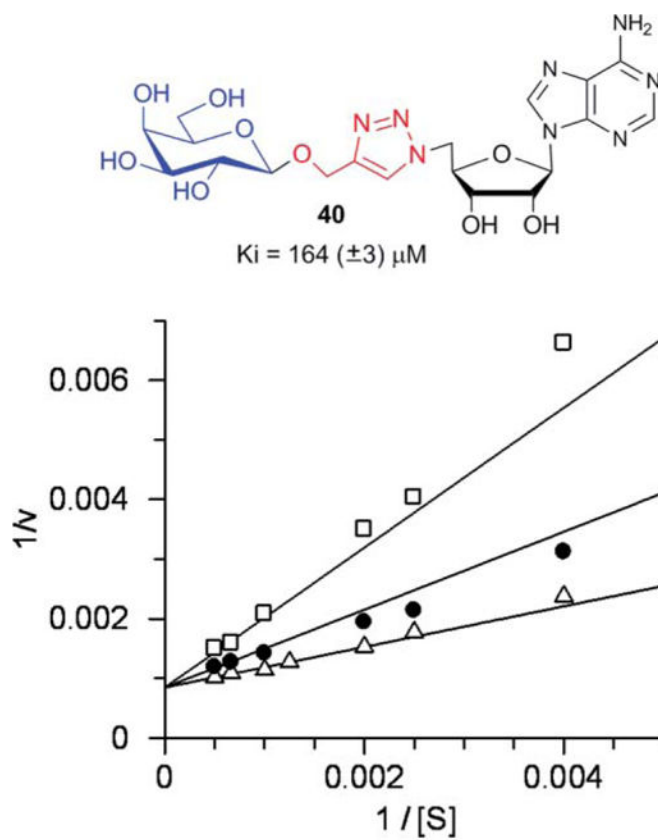
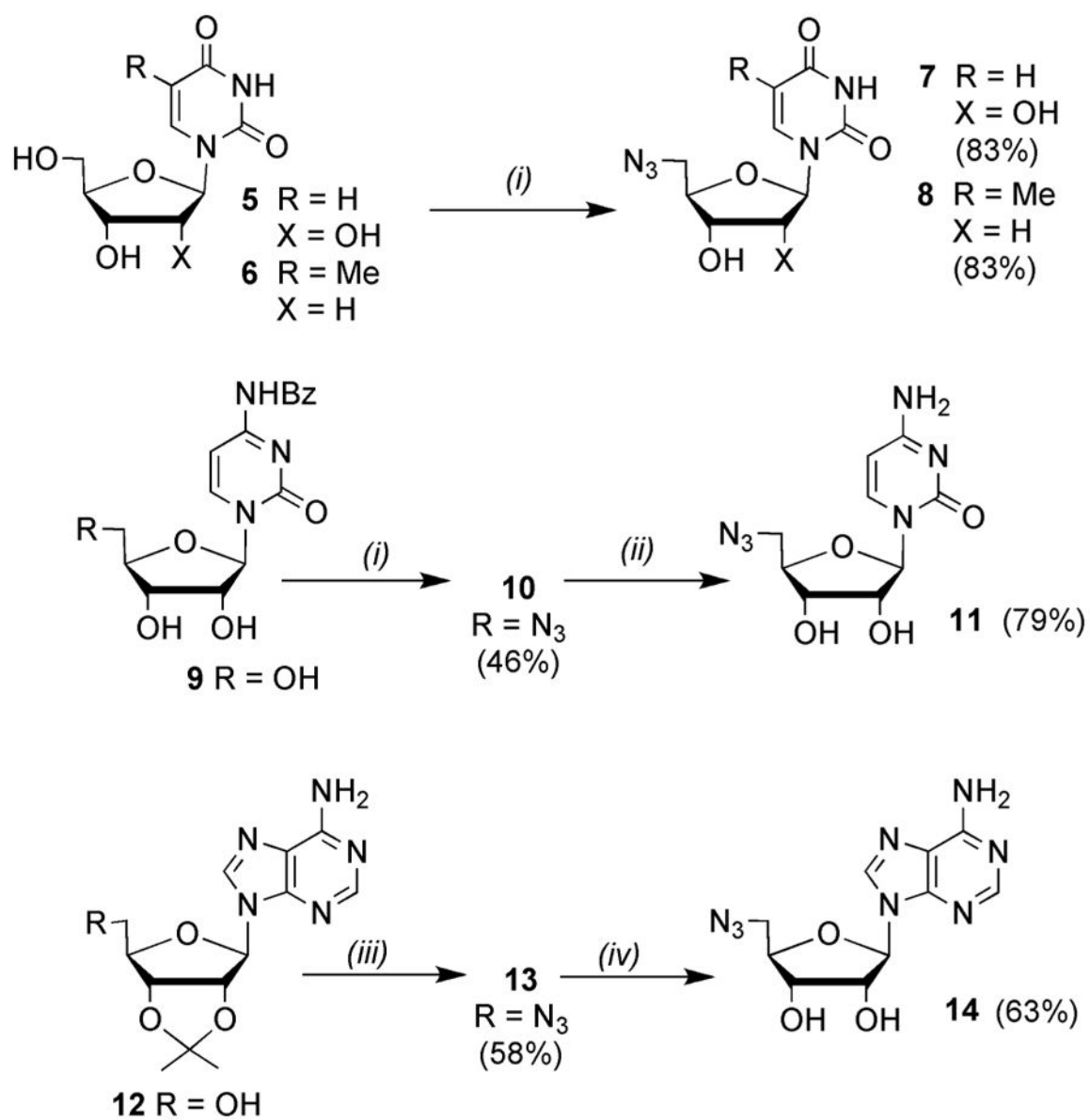
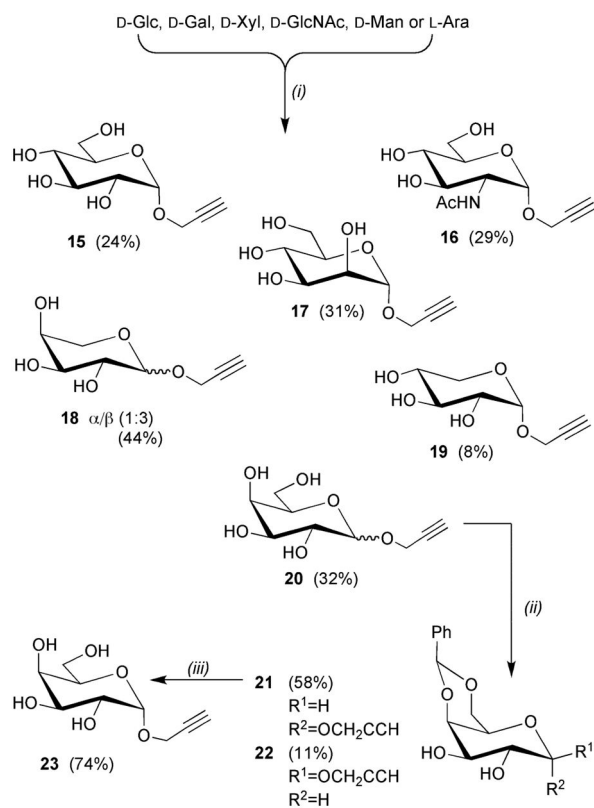


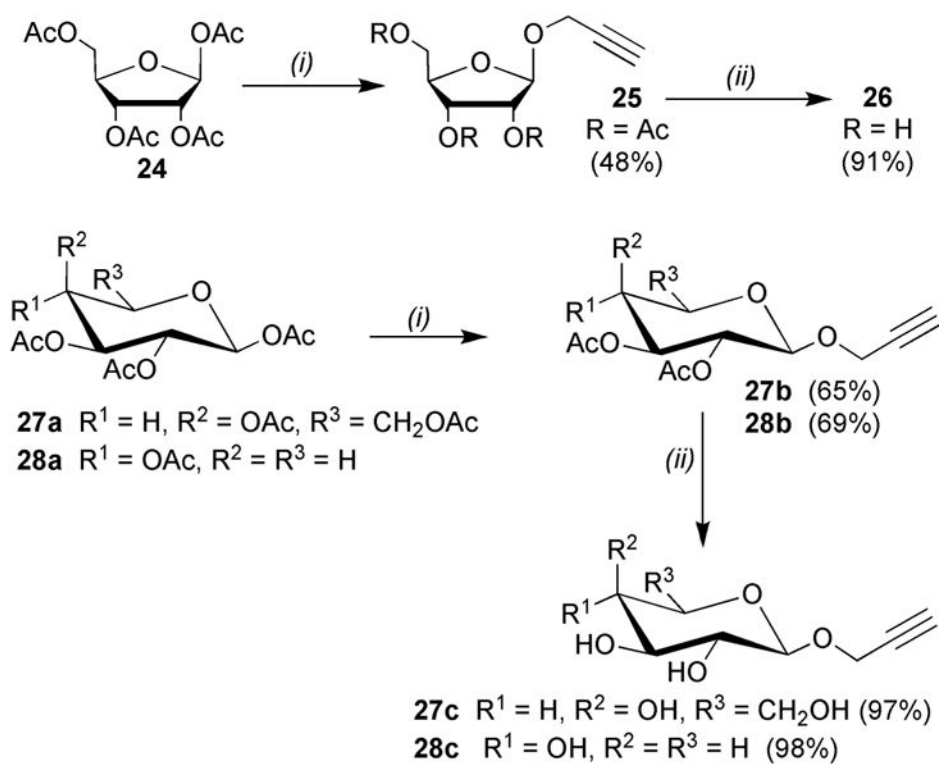
Fig. 3. Compound **40** as a competitive inhibitor of *BaPanK*. Double reciprocal plot of initial rate against ATP concentration in the presence of compound **40** at 0 μM (open triangles), 150 μM (closed circles) and 400 μM (open squares).

**Scheme 1.**

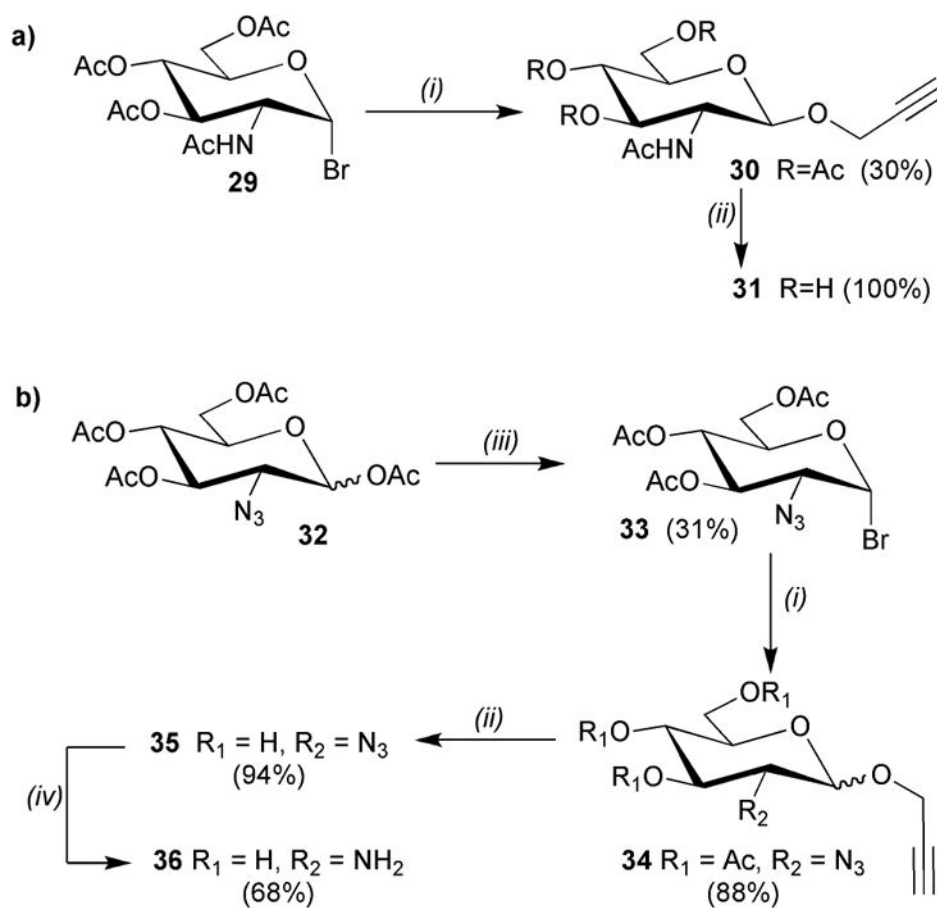
Reagents and conditions: (i) PPh₃, LiN₃, CBr₄, DMF, r.t., 3 days; (ii) conc. NH₄OH, MeOH, r.t., 6 days; (iii) PPh₃, DIAD, DPPA, THF, r.t., 68 h; (iv) TFA/H₂O (9:1), 0 °C–r.t., 25 min.

**Scheme 2.**

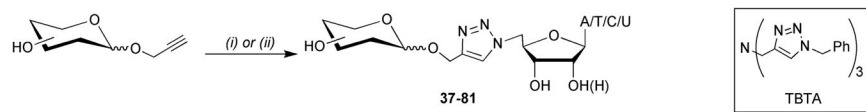
Reagents and conditions: (i) propargyl alcohol, AcCl (cat.), 100–120 °C, 1–3 days; (ii) PhCH(OMe)₂, TsOH, MeCN; (iii) AcOH(aq), 80 °C.

**Scheme 3.**

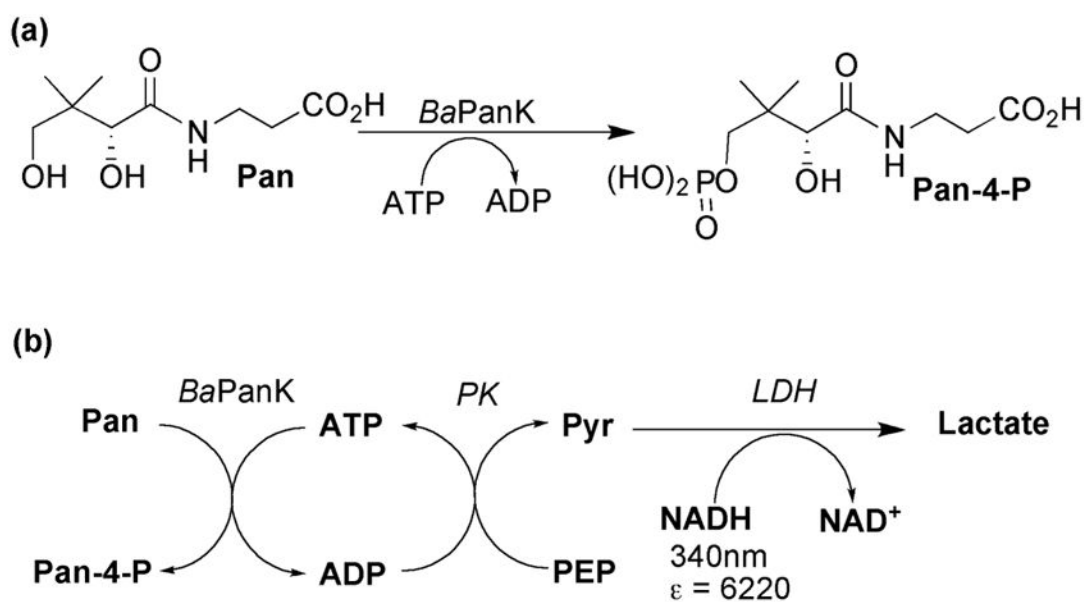
Reagents and conditions: (i) propargyl alcohol, BF₃·OEt₂, CH₂Cl₂, 0–20 °C; (ii) NaOMe, MeOH.

**Scheme 4.**

Reagents and conditions: (i) propargyl alcohol, AgOTf, 4Å molecular sieves, CH₂Cl₂, 0 °C, 2 h; (ii) NaOMe, MeOH; (iii) TiBr₄, CH₂Cl₂/EtOAc; (iv) Zn dust, NH₄Cl, EtOH/H₂O, 90 °C.

**Scheme 5.**

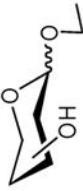
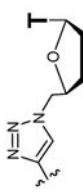
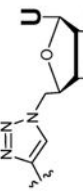
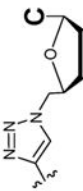
Reagents and conditions: (i) **8**, CuSO₄ (5 mol %), sodium ascorbate (10 mol %), MeOH/H₂O (3:1); (ii) **7** or **11** or **14**, CuBr (5 mol %), sodium ascorbate (10 mol %), TBTA (5 mol %), MeOH/H₂O/MeCN (1:1:1), r.t., sonication.

**Scheme 6.**

(a) *BaPanK* catalysed phosphorylation of pantothenate; (b) coupled assay used to monitor *BaPanK* activity; abbreviations: ADP = adenosine triphosphate, PK = pyruvate kinase, LDH = lactate dehydrogenase, PEP = phosphoenol pyruvate, Pyr = pyruvate.

Table 1

Compounds prepared and screened as inhibitors of *BaPanK*

								
	Yield (%)	% enzyme activity ^a	Yield (%)	% enzyme activity ^a	Yield (%)	% enzyme activity ^a	Yield (%)	% enzyme activity ^a
α -D-Glc	37 (72)	93	49 (61)	98	60 ^b (74)	96	71 (60)	90
β -D-Glc	38 (85)	95	50 (88)	91	61 (91)	99	72 (80)	104
α -D-Gal	39 (84)	97	51 (68)	80 ^b (68)	62 ^b (81)	105	73 (67)	— ^c
β -D-Gal	40 (82)	4	52 (54)	— ^c (63)	63 (87)	105	74 (70)	86
α -D-Man	41 (86)	84	53 (62)	108	64 (80)	94	75 (76)	105
α -D-Xyl	42 (88)	90	54 (60)	102	65 (94)	91	76 (82)	102
β -D-Xyl	43 (85)	90	55 (57)	100	66 (94)	91	77 (81)	100
α -D-GlcNAc	44 (80)	95	56 (82)	92	67 ^b (90)	102	78 (83)	109
β -D-GlcNAc	45 (53)	87	57 (49)	98	68 (76)	110	79 (68)	— ^c
L-Ara (α/β = 1:3)	46 (84)	76	58 (58)	104	69 (81)	— ^c (80)	80 (80)	91
β -D-Rib	47 (71)	95	59 (81)	100	70 (81)	83	81 (70)	107
D-GlcN (α/β = 1.1:1)	48 (48)	93						

^a Assays carried out in the presence of inhibitor (1 mM), ATP (125 μ M) and pantothenate (250 μ M). Percentage activity is relative to the same assay carried out in the absence of inhibitor.^b No further decrease in activity was observed when inhibitor concentration was increased to 2 mM.^c False positives (ie. inhibition of the PK/LDH coupled enzymes) in this assay.

Table 2NTP substrate kinetics with *BaPanK*

Substrate	K_m (μM)	k_{cat} (s^{-1})	k_{cat}/K_m ($\text{s}^{-1}\text{mM}^{-1}$)
ATP	510 (\pm 19)	1.5 (\pm 0.02)	2.9 (\pm 0.2)
dATP	138 (\pm 6)	0.9 (\pm 0.01)	6.6 (\pm 0.4)
dGTP	117 (\pm 13)	0.8 (\pm 0.02)	6.5 (\pm 0.9)
CTP	1759 (\pm 302)	1.5 (\pm 0.15)	0.9 (\pm 0.2)
dCTP	839 (\pm 91)	0.5 (\pm 0.02)	0.6 (\pm 0.1)
dTTP	723 (\pm 62)	0.4 (\pm 0.01)	0.5 (\pm 0.1)
UTP	1715 (\pm 155)	1.7 (\pm 0.06)	1.0 (\pm 0.1)

Author Manuscript

Author Manuscript

Author Manuscript

Author Manuscript